12-2008

A Three-Dimensional Pattern-Space Representation for Volumetric Arrays

William C. Barott
Embry-Riddle Aeronautical University, barottw@erau.edu

Paul G. Steffes
Georgia Institute of Technology

A Three-Dimensional Pattern-Space Representation for Volumetric Arrays

William C. Barott, *Member, IEEE* and Paul G. Steffes, *Fellow, IEEE*

***Abstract*— A three-dimensional pattern-space representation is presented for volumetric arrays. In this representation, the radiation pattern of an array is formed by the evaluation of the three-dimensional pattern-space on a spherical surface. The scan angle of the array determines the position of this surface within the pattern-space. This pattern-space representation is used in conjunction with a genetic algorithm to minimize the sidelobe levels exhibited by a thinned volumetric array during scanning.**

***Index Terms*—Antenna arrays, genetic algorithms**

I. Introduction

PHASED arrays are sometimes required to have a large aperture but a relatively small number of antennas. Placing these antennas at periodic intervals exceeding one half wavelength creates grating lobes in the radiation pattern and limits the usefulness of the array. Aperiodic placement techniques can remove grating lobes and minimize the sidelobe level of the array, as shown in Fig. 1 [1].

Theories of aperiodic arrays have been described in detail [2-3] and the usefulness of optimization algorithms in their design is well known. If the array steers the main beam over a variety of steering angles, a pattern-space evaluation can be used to determine the worst-case sidelobe levels in a single step, as opposed to evaluating all possible radiation patterns individually [1, 4]. This technique reduces the number of dimensions required in the analysis, greatly improving the speed of these algorithms. Although the design of aperiodic linear and planar arrays has been well-explored, little attention has been given to the design of aperiodic volumetric arrays. This is due partially to the lack of an effective pattern-space representation for volumetric arrays.

In certain applications, volumetric arrays are preferred over planar or linear arrays. For example, planar and linear arrays exhibit main-beam broadening when steered toward the end-fire direction of the array. These arrays may be unsuitable for applications requiring the array to exhibit a constant beam shape. On the other hand, volumetric arrays can maintain a constant main-beam resolution regardless of steering angle.

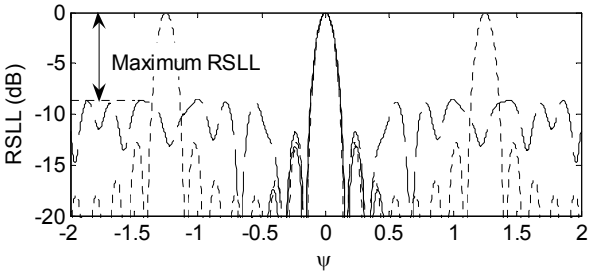

Fig. 1. Radiation patterns illustrating grating lobe reduction. Sidelobe level relative to the main lobe (RSLL) is plotted for an array of 15 elemental antennas with 0.4 wavelength spacing (solid), 8 elemental antennas with 0.8 wavelength spacing (dot) and 8 elemental antennas with aperiodic spacings occupying the same aperture (dash).

We present a three-dimensional representation of the pattern-space of a volumetric array. It is shown that the radiation pattern of a volumetric array is found by evaluating the pattern-space on a spherical surface. The position of this surface within the pattern-space is determined by the steering angle of the array. This pattern-space representation is integrated with an optimization algorithm to minimize the sidelobe levels exhibited by an aperiodic volumetric array during scanning. Some results from this algorithm are presented at the conclusion of this paper.

II. Derivation of the Pattern-Space

A. Deriving the Pattern-Space Representation

The pattern-space of an array is obtained by examining the mathematical form of the beamformer. The beamformer is given by $\mathbf{y} = \mathbf{a}^H \mathbf{x}$, where $\mathbf{y}$ is the output beam and $\mathbf{a}^H$ is the Hermitian (complex transpose) of the steering vector. The vector $\mathbf{x}$ consists of the antenna phasors written as

$$\mathbf{x}_i = \exp\left[jk \left(X_i \cos\phi \sin\theta + Y_i \sin\phi \sin\theta + Z_i \cos\theta \right) \right], \qquad (1)$$

where $k = 2\pi/\lambda$, ϕ and θ represent the angle of arrival of a signal, and X_i, Y_i, and Z_i represent the position of the i_{th} elemental antenna out of N total antennas.

Using primed angles to indicate the steering direction, the

Manuscript received April 23, 2007.

William C. Barott: Embry-Riddle Aeronautical University, Electrical and Systems Engineering Department, Daytona Beach, FL, 32127 USA (email william.barott@erau.edu)

Paul Steffes: Georgia Institute of Technology, School of Electrical and Computer Engineering, Atlanta, GA 30332 USA

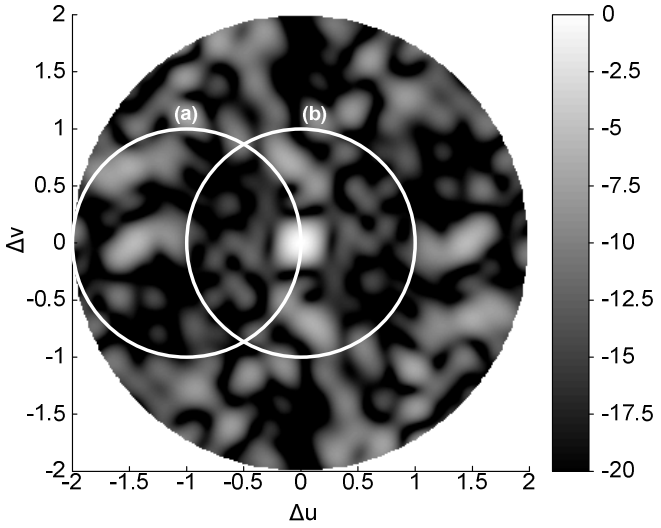

Fig. 3. Pattern-space representation for a planar array. The circles indicate the pattern exhibited by the array when it is steered to the horizon (a) and to zenith (b). Plotted for a 5x5 array with 0.75λ average spacing between antennas. The color scale is from -20 to 0 dB relative to the main lobe.

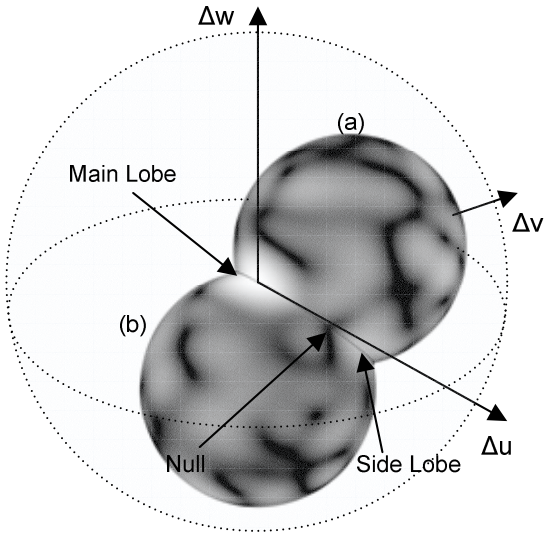

Fig. 4. Pattern-space representation for a volumetric array. Two spheres intersect the main lobe at the origin, and indicate patterns for an array steered to the horizon (a) and the same array steered to zenith (b). Plotted for a 3x3x3 array with 0.75λ average spacing between antennas. Uses the same color scale as Fig. 3. Indicated features correspond to those in Fig. 5. The dotted arcs indicate the pattern-space boundary and an equatorial arc.

steering vector is written as

$$\mathbf{a}_i^H = \exp\left[-jk\left(X_i \cos\phi' \sin\theta' + Y_i \sin\phi' \sin\theta' + Z_i \cos\theta'\right)\right]. \quad (2)$$

Abbreviating the functions $c_\theta = \cos\theta$ and $s_\theta = \sin\theta$ and writing the beamformer yields

$$\mathbf{y} = \sum_{i=1}^{N} \exp\left\{ jk\left[\begin{array}{r} X_i\left(c_\phi s_\theta - c'_\phi s'_\theta\right) + Y_i\left(s_\phi s_\theta - s'_\phi s'_\theta\right) \\ + Z_i\left(c_\theta - c'_\theta\right) \end{array} \right] \right\}. \quad (3)$$

In the case of a linear array positioned on the Y axis, the equation simplifies to

$$\mathbf{y} = \sum_{i=1}^{N} \exp\left\{ jk\left[Y_i\left(s_\phi - s'_\phi\right)\right]\right\}. \quad (4)$$

The pattern-space representation for a linear array is obtained from the substitution $\Psi = s_\phi - s'_\phi$ [5], which has the range $\Psi = -\left(s'_\phi \pm 1\right)$ for a total range of ± 2. The magnitude of (4) is symmetric about the main beam at $\Psi = 0$. Fig. 1 contains examples of patterns-space representations of linear arrays. Evaluating (4) between $\Psi = 0$ and $\Psi = 2$ yields the worst-case sidelobe level exhibited by the array for all possible scan angles. Without a pattern-space representation, it is necessary to evaluate the radiation pattern at many steering angles to determine the worst-case sidelobe levels.

B. Planar and Volumetric Arrays

In the case of a planar array located in the XY plane, the output of the ideal beamformer is given by

$$\mathbf{y} = \sum_{i=1}^{N} \exp\left\{ jk\left[X_i\left(c_\phi s_\theta - c'_\phi s'_\theta\right) + Y_i\left(s_\phi s_\theta - s'_\phi s'_\theta\right)\right]\right\}. \quad (5)$$

By defining the pattern-space $\Delta u = c_\phi s_\theta - c'_\phi s'_\theta$ and $\Delta v = s_\phi s_\theta - s'_\phi s'_\theta$, the maximum extent of these variables is the circle $\Delta u^2 + \Delta v^2 = 4$. For any steering angle, the radiation pattern is defined by a circle of radius 1 within the pattern-space, as shown in Fig. 3.

In previous work (see e.g. [1]) pattern-space optimization of aperiodic arrays was applied only to linear and planar arrays. Although randomly distributed volumetric arrays have been demonstrated [6], pattern-space representations and optimization algorithms have not been applied.

The pattern-space of a volumetric array is found by rewriting the ideal beamformer as

$$\mathbf{y} = \sum_{i=1}^{N} \exp\left[jk\left(X_i \Delta u + Y_i \Delta v + Z_i \Delta w\right)\right], \quad (6)$$

where $\Delta w = c_\theta - c'_\theta$. The maximum extent of the pattern-space is defined in the volume $\Delta u^2 + \Delta v^2 + \Delta w^2 = 4$. For any steering angle, the radiation pattern is evaluated on the surface of a sphere that intersects the origin and has a radius of 1, as shown in Fig. 4. The steering angle determines the center of this spherical surface within the pattern-space. Consequently,

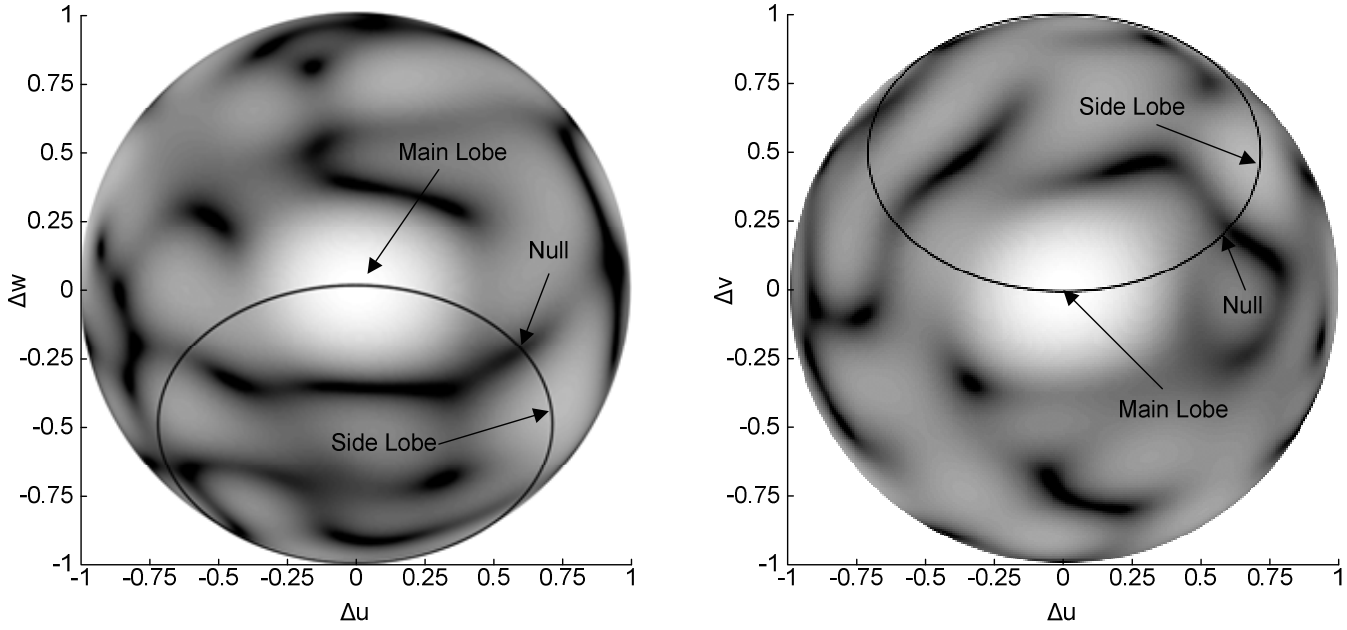

Fig. 5. Planar projections of the pattern-space of the volumetric array from Fig. 4, evaluated for the hemispheres containing the main lobe. (Left) A uw projection for the radiation pattern when the array is steered toward the horizon. (Right) A uv projection for the radiation pattern when the array is steered to zenith. The black ellipse corresponds to the curve where the two radiation patterns intersect in uvw space. The two radiation patterns exhibit the same values for points on this ellipse. Easily recognized features include the strong sidelobe and its neighboring null, which are indicated on the plots.

the radiation pattern of volumetric arrays changes dramatically during beam steering as opposed to cases with planar or linear arrays. Grating lobes contained within the volume are exhibited only when the surface of the radiation pattern intersects the lobe.

Fig. 5 contains planar projections of the radiation pattern of the array from Fig. 4. These plots correspond to the cases when the main beam is steered toward the horizon and to zenith. These projections show the characteristic change in the radiation pattern of a volumetric array for different steering angles. Additionally, these projections demonstrate the required similarity at points where the spherical shells of these radiation patterns intersect in pattern-space. The black ellipses indicate the curve corresponding to this intersection. Several features are easily recognized, including a high sidelobe and a nearby null. These features are also visible in the perspective plot in Fig. 4.

C. Consistency Between Pattern-Spaces

A three-dimensional pattern-space is counterintuitive because radiation patterns are evaluated only along two look-angles (ϕ and θ). However, the three-dimensional representation is consistent with this requirement and with the pattern-space representations of planar and linear arrays. For example, for an array confined to the XY plane, the three-dimensional pattern-space is independent of Δw. Projecting the pattern-space in Fig. 4 onto the uv plane yields the pattern-space representation used for planar arrays (as in Fig. 3).

III. Optimizing Volumetric Arrays

A. Genetic Algorithm

The three-dimensional pattern-space representation was integrated with a genetic algorithm (GA) to minimize the sidelobe levels of an aperiodic volumetric array. The usefulness of genetic algorithms as optimization tools is well known and they have been applied successfully to aperiodic linear and planar array design for more than a decade [1, 7].

The basic processes of a GA are shown in Fig. 6. The GA employed in this study implements the concepts of mutation and crossover. The algorithm allows mutation to alter genes by up to ten percent during each generation. The GA terminates after 20 generations without improvement, and each trial is repeated many times to ensure statistical reliability of the results. The fitness of individuals within the algorithm was defined by the inverse of the maximum relative sidelobe level, or –RSLL [1]. The algorithm maximizes the fitness of the population.

B. Optimization Model

The GA represented arrays using the model shown in Fig. 7, which is similar to that presented in [4]. The antenna positions are optimized with respect to their proximal grid points, which are distributed throughout the aperture at intervals of S. Antenna positions are described by continuous variables representing the offset from the proximal grid point, rather than Boolean values describing the presence or absence of an

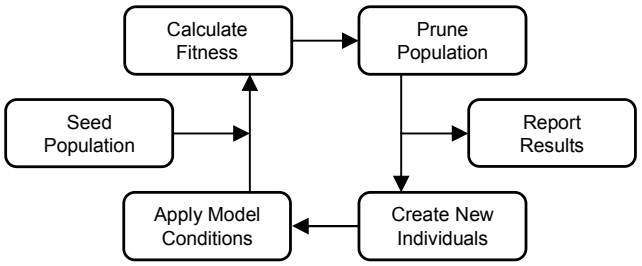

Fig. 6. Genetic algorithm processes.

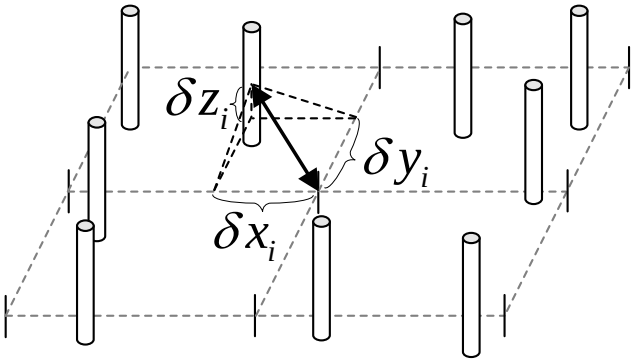

Fig. 7. The aperiodic array model used in this study. The difference between the position of an antenna and its proximal grid point is indicated by δx, δy, and δz.

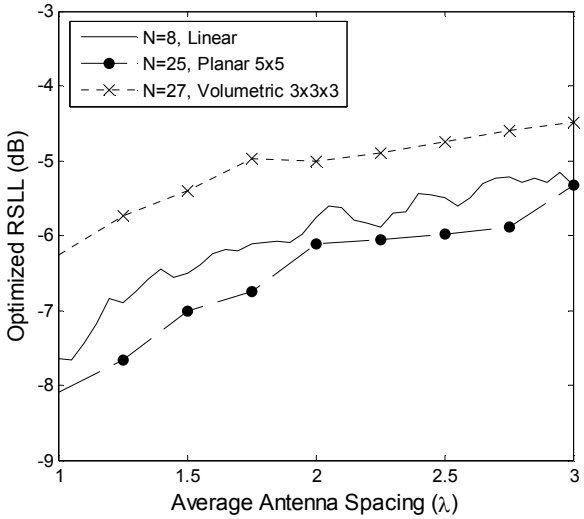

Fig. 7. Sidelobe levels versus antenna spacing for the linear, planar, and volumetric arrays. Although the 27-element volumetric arrays have more antennas than the 8-element linear and 25-element planar arrays, the volumetric arrays exhibit higher maximum sidelobes.

antenna at a grid point. The number of antennas and the spacing between the grid points are defined prior to the execution of the algorithm.

C. Optimization Results

The algorithm was used to optimize an aperiodic volumetric array consisting of 27 elements in a 3x3x3 configuration. The spacing between adjacent grid points was varied between λ and 3λ. Fig. 7 shows the results of this optimization. Data from the optimization of an 8-element linear array and a 25-element planar array are included for comparison. In each case, the arrays were optimized in pattern space for operation over all possible steering angles. The distance between adjacent grid points was the same in each dimension (X, Y, Z).

The optimized sidelobes of the 27-element volumetric array are between 1dB and 2dB higher than those for the 25-element planar array having the same spacing between adjacent gridpoints, and about 1dB higher than those for the linear array containing only 8 elements. This is due to the increased complexity of the pattern-space of the volumetric array.

IV. Conclusions

The three-dimensional pattern-space is an effective and accurate representation of the radiation pattern exhibited by a volumetric array. When this pattern-space representation is implemented in an optimization algorithm, the computational cost of the algorithm is significantly reduced. For example, if an array requires M sample points along each coordinate axis (u, v, w) to adequately determine the worst-case sidelobe level, the algorithm must evaluate M^3 discrete samples of the pattern-space. If the pattern-space representation is not used and many individual radiation patterns are calculated and analyzed, approximately M^4 discrete samples are required.

The optimized sidelobes of a volumetric array were found to be higher than those of a similar planar array. However, volumetric arrays are preferred over planar arrays in applications requiring the array to present a constant beam-shape throughout a wide range of steering angles. Future work involves analysis of volumetric arrays having a large number of antennas and extending this analysis to conformal arrays.

References

[1] R. L. Haupt, "Thinned arrays using genetic algorithms," *IEEE Trans. Antennas Propag.*, vol. 42, pp. 993-999, July 1994.

[2] Y. Lo, "A mathematical theory of antenna arrays with randomly spaced elements," *IEEE Trans. Antennas Propag.*, vol. 12, pp. 257-268, May 1964.

[3] A. Ishimaru, "Theory of unequally-spaced arrays," *IEEE Trans. Antennas Propag.*, vol. 10, pp 691-702, Nov. 1962.

[4] M. G. Bray, D. H. Werner, D. W. Boeringer, and D. W. Machuga, "Optimization of thinned aperiodic linear phased arrays using genetic algorithms to reduce grating lobes during scanning", *IEEE Trans. Antennas Propag.*, vol. 50, pp. 1732-1742, Dec. 2002.

[5] R. C. Hansen, Phased Array Antennas, New York: Wiley, 1998.

[6] A. Tennant, A. F. Fray, D. B. Adamson and M. W. Shelley, "Beam scanning characteristics of 64 element broadband volumetric array," Electronics Letters, vol. 33, pp. 2001-2002, 20 Nov. 1997.

[7] R. L. Haupt, "An introduction to genetic algorithms for electromagnetics," *IEEE Antennas Propag. Mag.*, vol. 37 pp. 7-15, April 1995.